Magnetic composites Fe_3O_4@SiO_2@PILs as sorbents for efficient denitrogenation of fuel oil

Feng Wang[1], Jie Li[1], Long Xu[1], Feng Jiang[2], Jianfeng Zhang[1] ✉

[1]*Faculty of Materials Science and Chemical Engineering, Ningbo University, Ningbo 315211, People's Republic of China*
[2]*Department of Pharmacy, Gannan Medical University, Ganzhou 341000, People's Republic of China*
✉ *E-mail: zjf@nbu.edu.cn*

Published in Micro & Nano Letters; Received on 16th April 2019; Revised on 7th August 2019; Accepted on 21st August 2019

In this work, the study of synthesis and denitrogenation of magnetic polymeric ionic liquids (PILs) for N-compounds in simulated oils and diesel are reported. Three functionalised magnetic particles, Fe_3O_4@SiO_2@PILs with side alkyl chain of C2, C4 and C6, respectively, were prepared by grafting PILs on the surface of silica-coated Fe_3O_4. Fourier transform infrared spectra, thermogravimetric analysis, X-ray diffraction and scanning electron microscopy were carried out to characterise the structure of Fe_3O_4@SiO_2@PILs. It has shown that Fe_3O_4@SiO_2@ PILs possess precious merits for sorbents, such as regular morphology, good stability and magnetic properties. Denitrogenation experiments of simulated oils demonstrate that Fe_3O_4@SiO_2@ PILs show better denitrogenation efficiency of basic N-compounds than neutral N-compounds. The effects of temperature, reaction times, ratio of reagent to oil on denitrogenation for simulated oils were explored, and 92.1% denitrogenation efficiency was obtained to remove quinoline from simulated oils. Denitrogenation of Fe_3O_4@SiO_2@PILs in diesel leads to 84.3% denitrogenation efficiency, and it can remain 82.5% denitrogenation efficiency after five times of recycles. Compared with other similar sorbents, Fe_3O_4@SiO_2@PILs show competitive performances to eliminate organic N-compounds. It is hopeful that Fe_3O_4@SiO_2@PILs can be promising sorbents for purification of liquid fuel by adsorptive denitrogenation.

1. Introduction: N-compounds in fuel can be changed into NO_x during combustion which has an incalculable impact on the environment [1–3]. In addition, in the process of hydrodesulphurisation, N-compounds will reduce the thermal and oxidative stability of diesel. Therefore, denitrogenation from oils have attracted extensive attentions of both academic and industrial communities.

Hydrodenitrogenation (HDN) is an effective and widely used technology for the elimination of N-compounds in petroleum refining processes [4, 5]. However, HDN process requires tough operating conditions (such as noble catalyst, high pressure and high temperature). Adsorptive denitrogenation (ADN) [6–8] is the alternative method to the elimination of N-compounds from oils with high removal capacity, convenient operation, low cost and possibility of materials recycling. Activated carbon [9, 10], molecular surface imprinted polymers [11, 12], microporous or mesoporous materials [13–15] and metal–organic frameworks materials [16–18] are reported as ADN sorbent in recent years.

Ionic liquids (ILs) [19, 20] which are composed of an organic cation and an inorganic or organic anion were applied in the area of denitrogenation. Wang and co-workers [21] utilised [Bmim]Cl/$ZnCl_2$ in extraction of denitrogenation with an efficiency of 93.8% (carbazole) and 98% (pyridine), respectively. Maschmeyer and his co-workers [22] applied various ILs based on common cations and anions as extractants to study the denitrogenation of pyridine and indole from a simulated oil. The results demonstrated that the sizes of cation and anion are the major factors to the efficiency of N-compound extraction. Liu *et al.* [23] researched the denitrogenation efficiency of $H_2PO_4^-$-based IL to the simulated oils, and the mechanism of denitrification ascertained that a liquid–liquid extraction as well as the acidity of ILs both contribute to denitrogenation. Polymeric ionic liquids (PILs) [24–26], assembled by connecting IL species in their repeated units of polymer chains, can be functionalised with unique properties, such as designable structure, strong polarity, adjustable physicochemical properties, thermal and chemical stability, which is suitable for the promising candidates as sorbents of denitrogenation. However, it is difficult to recycle the powdered adsorbents after treatment.

Magnetic solid phase adsorption (MSPA) [27, 28] is a novel simple and effective method for sample purification due to their properties of easy automatic operation and low consumption of organic reagents. Sun and co-workers [29] prepared magnetic HKUST-1/Fe_3O_4 composites to remove the N-compounds in fuel, which showed that the adsorbents had a high adsorptive capacity of 0.89 mmol/g N in indole. Afzalinia and his colleagues [30] synthesised Fe_3O_4@TMU-17-NH_2 as sorbent for highly efficient ultrasonic-assisted denitrogenation of fossil fuel. The maximum adsorption capacity of the synthesised composite to indole and quinoline is calculated by 375.93 and 310.18 mg/g at 25°C, respectively.

In this work, magnetic sorbents, MSPA-coupled PILs, were proposed for the denitrogenation of N-compounds. PILs were prepared on the surface of silica-core shell Fe_3O_4 which was modified by 3-mercaptopropyltrimethoxysilane (MPTMS) for MSPA. The sorbents were applied for rapid separation of N-compounds from the simulated oils and real oils.

2. Experimental section

2.1. Materials: All chemical regents were used without any further purification (Table 1). 1-Vinylimidazole, 1,2-dibromoethane, 1,4-dibromobutane, 1,6-dibromohexane, quinoline, indole, sodium acetate and acetonitrile were purchase from Shanghai Aladdin. $FeCl_3{\cdot}6H_2O$, ethyl acetate, azobisisobutyronitrile (AIBN), carbazole, $FeCl_2.4H_2O$, MPTMS, tetraethoxysilane (TEOS) and pyridine were purchased from Macklin Reagent.

2.2. Characterisation: ^{1}H NMR and ^{13}C NMR spectra were recorded by a Varian MERCURY Plus-400 MHz spectrometer. Fourier transform infrared spectra were carried out on Nicolet 6700 spectrometer. X-ray diffractometer with Cuka radiation was used to record the structural characteristics of the adsorbents. Thermal gravimetric analysis (TG) was performed with a SII TG/DTA 6300. The microstructure of nanomaterials was observed by scanning electron microscopy (SEM, Hitachi TM 3000). Magnetic hysteresis was carried out on a quantum design

© The Institution of Engineering and Technology 2019

Table 1 Reagents and chemicals

Chemicals	Purity level, %	CAS number
1-vinylimidazole	99.9	1072-63-5
1,2-dibromoethane	99	1106-93-4
1,4-dibromobutane	98	1110-52-1
1,6-dibromohexane	97	6629-03-8
indole	99.5	775-05-8
MPTMS	95	4420-74-0
quinoline	99	91-22-5
AIBN	99	78-67-1
$FeCl_3.6H_2O$	98	10025-77-1
$FeCl_2.4H_2O$	99.9	13478-10-9
TEOS	98	681-84-5
carbazole	99	127-09-3
pyridine	99.5	67-64-1

superconducting quantum interference device magnetometer. Nitrogen content was measured by TN-3000 series nitrogen analyser.

2.3. Preparation of Fe_3O_4@SiO_2@PILs

2.3.1. Synthesis of bis-vinyl imidazolium dibromide salts: The bis-vinyl imidazolium dibromide salts were synthesised via the reaction of 1-vinylimidazole (0.5 mol) and 1,2-dibromoalkane (0.25 mol) dissolved in 100 ml acetonitrile at 80°C for 48 h (Fig. 1). The product was washed with diethyl ether and ethyl acetate three times and then dried under dynamic vacuum at room temperature for 24 h at 40°C.

1,6-bis(1-vinylimidazolium)hexane bromide (1): ^{1}H-NMR (400 MHz, D_2O) δ 7.66 (d, 2H), 7.47 (d, 2H), 7.03 (dd, 2H), 5.69 (dd, 2H), 5.31 (dd, 2H), 4.13 (t, 4H), 1.79 (p, 4H), 1.26 (p, 4H).

^{13}C-NMR (101 MHz, D_2O) δ 134.29, 128.23, 122.84, 119.48, 109.31, 49.79, 28.89, 24.85.

1,4-bis(1-vinylimidazolium)butane bromide (2): ^{1}H-NMR (400 MHz, D_2O) δ 7.64 (d, 2H), 7.44 (d, 2H), 6.99 (dd, 2H), 5.71–5.61 (m, 2H), 5.32–5.24 (m, 2H), 4.16 (d, 4H), 1.82 (q,, 4H).

^{13}C-NMR (101 MHz, D_2O) δ 134.39, 128.10, 122.64, 119.60, 109.41, 49.01, 25.99.

1,2-bis(1-vinylimidazolium)ethane bromide (3): ^{1}H-NMR (400 MHz, D_2O) δ 7.74 (d, 2H), 7.47 (d, 2H), 7.03 (dt, 2H), 5.71 (dd, 2H), 5.39–5.31 (m, 2H), 4.74 (*d*, J = 1.9 Hz, 4H).

^{13}C-NMR (101 MHz, D_2O) δ 134.89, 127.95, 122.74, 120.43, 110.42, 48.85.

2.3.2. Preparation of Fe_3O_4: Fe_3O_4 was prepared as reported method [27]. In short, 5.41 g $FeCl_3{\cdot}6H_2O$ and 1.98 g $FeCl_2{\cdot}4H_2O$ were dissolved in 50 ml deionised water, then 2 ml of hydrazine hydrate and 10 ml of 30% ammonia were successively added to the system. The mixture was heated to 90°C by stirring for 1 h, and 4.2 g of sodium acetate was added for further stirring for 10 min. The product was collected via magnetic separation and washed with water and acetone for several times.

2.3.3. Preparation of Fe_3O_4@SiO_2-SH: Fe_3O_4@SiO_2-SH was prepared by sequential silylanisation on the surface of Fe_3O_4. The mixture of 5 g Fe_3O_4, 10 ml TEOS and 20 ml MPTMS was stirred for 8 h at room temperature. The Fe_3O_4@SiO_2-SH was collected by a magnet, and the residual reactants were removed by ultrasonic washing with water for several times and then dried under vacuum at 40°C overnight.

2.3.4. Preparation of Fe_3O_4@SiO_2@PILs: Fe_3O_4@SiO_2@PILs were prepared as the method reported in the literature [31]. Shortly, Fe_3O4@SiO_2-SH (5 g), the bis-vinyl imidazolium salt (27.5 mmol), AIBN (0.2 g) and 200 ml of ethanol were added in a three-necked round bottom flask. The mixture was stirred for 48 h at 80°C under nitrogen atmosphere. The obtained composite was washed with methanol and diethyl ether, respectively.

The above composite was dispersed in 10 ml of water, and 2 ml of H_2SO_4 was added into the mixtures by keeping the mixture in a low temperature. The reaction was carried on for 24 h by stirring at room temperature. Then Fe_3O_4@SiO_2@PILs were separated and washed by water to remove H_2SO_4, dried in an oven at 60°C overnight (Fig. 2).

2.4. Adsorption procedure: In adsorption study, simulated oils were composed by dissolving a certain amount of N-compound (such as quinoline, pyridine, indole and carbazole) in a mixing solution of toluene (80 wt. %) and n-heptane (20 wt. %), respectively. Real fuel was provided by Sinopec Zhenhai Refining & Chemical Company, with a content of 250 ppm nitrogen element (wt.).

About 0.5 g of Fe_3O_4@SiO_2@PILs was added to 5.0 ml of simulated oils, and the mixture was stirred to reach adsorption balance. After the adsorption completed, the Fe_3O_4@SiO_2@PILs was separated from oils solution by an external magnetic field and the nitrogen content of the simulated oils was measured by TN-3000 series nitrogen analyser. The efficiency of extraction E(%) was determined according to (1), where c_i and c_f are the abbreviation of initial and final concentrations in the studied molecule, respectively

$$E(\%) = \frac{c_i - c_f}{c_i} \times 100 \quad (1)$$

The regeneration of Fe_3O_4@SiO_2@PILs can be managed in the common regeneration process of ILs. In brief, after completion of denitrogenation, Fe_3O_4@SiO_2@PILs were separated by magnet and then washed by ethyl acetate and water, each for five times,

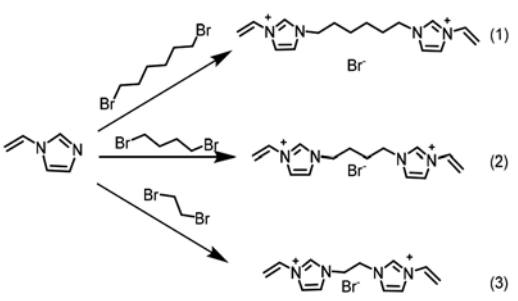

Fig. 1 *Synthesis routes of bis-vinyl imidazolium dibromide salts*

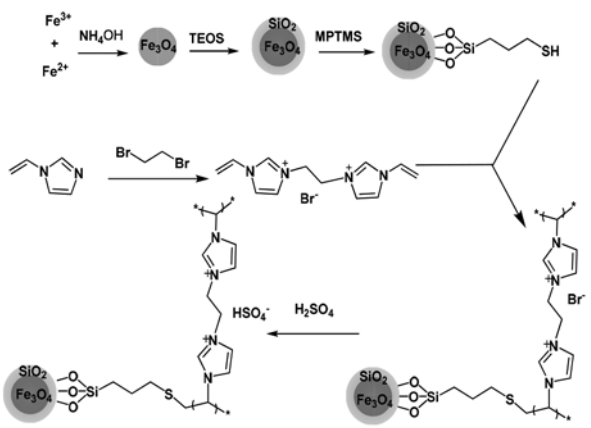

Fig. 2 *Preparation process of Fe_3O_4@SiO_2@PILs*

© The Institution of Engineering and Technology 2019

doi: 10.1049/mnl.2019.0245

respectively. Finally, Fe_3O_4@SiO_2@PILs were added to the aqueous solution of sulphuric acid for regeneration.

3. Results and discussion

3.1. Characterisation of Fe_3O_4@SiO_2@PILs: Fig. 3 demonstrated the FTIR spectra of Fe_3O_4, Fe_3O_4@SiO_2-SH and Fe_3O_4@SiO_2@PILs. The peaks at 590 and 1086 cm^{-1} are attributed to the stretching vibrations of Fe–O bond and Si–O bond, respectively. The peak of 2420 cm^{-1} corresponds to the SH stretching vibration. The acidic counter-anion HSO_4^- appears at the position of 1203 and 1149 cm^{-1}, respectively, verifying the asymmetric and symmetric stretching vibration of O = S = O [32]. The peak of 850 cm^{-1} assigned to the C–H in-plane vibration of imidazolium ring. The C–H bond of the alkyl chain in the imidazolium ring appears at 2800–3000 cm^{-1} for Fe_3O_4@SiO_2@PIL-C_2, Fe_3O_4@SiO_2@PIL-C_4 and Fe_3O_4@SiO_2@PIL-C_6, respectively, indicating that, with the increase of the base chain, the stretching vibration peak of methylene of alkyl chain appears gradually obvious.

The thermogravimetric analysis (TGA) curves are illustrated in Fig. 4. The weight loss process can be classified into three stages: the first stage was from 30 to 200°C, mainly resulted from the moisture evaporation on the surface of the hygroscopicity of these composites. The second stage was in the range of 200–380°C, where the weight loss may be caused by the decomposition of the ILs with the sulfhydryl group and double bond polymerisation, therefore the loading capacity of PILs in Fe_3O_4@SiO_2@PILs is calculated by 15–20% which is in line with the estimated value according to the reactions. The third stage was from 380 to 800°C, which can be attributed to the Fe_3O_4 changes to Fe_2O_3 in phase transfer and the decomposition of SiO_2. The TGA analysis demonstrates that the synthesised Fe_3O_4@SiO_2@PILs can be stable at normal circumstances for practical application.

Fig. 5 shows the magnetisation curves of Fe_3O_4, Fe_3O_4@SiO_2-SH and Fe_3O_4@SiO_2@PILs. The saturation magnetisation of Fe_3O_4 is

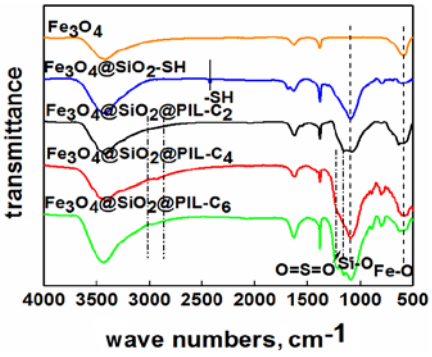

Fig. 3 *FTIR spectra of Fe_3O_4, Fe_3O_4@SiO_2-SH and Fe_3O_4@SiO_2@PILs*

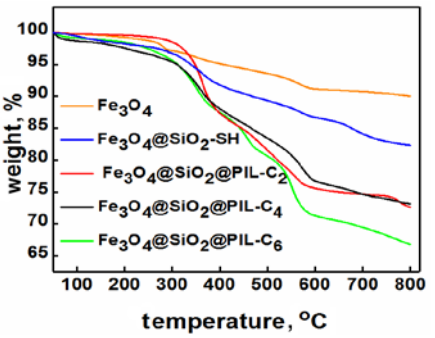

Fig. 4 *TGA curves of Fe_3O_4, Fe_3O_4@SiO_2-SH and Fe_3O_4@SiO_2@PILS*

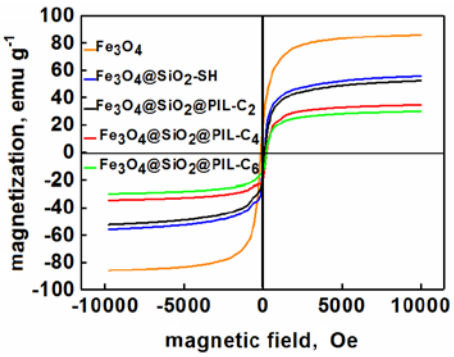

Fig. 5 *Magnetic hysteresis curves of Fe_3O_4, Fe_3O_4@SiO_2-SH, Fe_3O_4@SiO_2@PILs*

86.1 emu g^{-1}, and saturation magnetisation decreases with the increase of the modified molecules. The saturation magnetisation of Fe_3O_4@SiO_2-SH, Fe_3O_4@SiO_2@PIL-C_2, Fe_3O_4@SiO_2@PIL-C_4 and Fe_3O_4@SiO_2@PIL-C_6 were 55.8, 52.4, 34.6 and 30.0 emu g^{-1}, respectively, which reveals that the magnetism of the magnetic composites is sufficient for the magnetic separation.

The X-ray diffraction (XRD) patterns of Fe_3O_4, Fe_3O_4@SiO_2-SH and MPs were illustrated in Fig. 6. All the diffraction peaks verify the cubic inverse spinel Fe_3O_4, which indicates that the Fe_3O_4 particles are encapsulated in cages of PILs. Therefore, the preparation of the expected composite was confirmed by XRD studies.

The SEM images were used to illustrate the morphologies of the prepared composites. As shown in Fig. 7, both Fe_3O_4 and Fe_3O_4@SiO_2-SH have spherical nanoparticles structure in average size of 40 and 230 nm, respectively, while Fe_3O_4@SiO_2@PILs are ultrafine particles in diameter of 30–50 µm. The size of the three composites is in the order of Fe_3O_4@SiO_2@PIL-C_4 > Fe_3O_4@SiO_2@PIL-C_6 > Fe_3O_4@SiO_2@PIL-C_2, which complies to the fact that the PILs size changes slightly with the increasing of the alkyl chain length connected on the imidazole ring.

3.2. Denitrogenation efficiency of different N-compounds: The comparison of denitrogenation efficiency to different N-compounds in simulated oils is shown in Table 2. It can be seen from Table 2 that the synthesised adsorbents perform better denitrogenation efficiency of basic N-compounds than that of neutral N-compounds.

The possible mechanism (Fig. 8) is assumed that H^+ from the ionisation of HSO_4^- anions ILs can attack lone pair of electrons of N in the quinoline molecule to form charged ions to accelerate the transfer of quinoline from oil phase into aqueous phase, which agrees to the denitrification mechanism of $H_2PO_4^-$ anion imidazolium-based ILs in the literature [22, 23, 30]. On the other hand, the π–π interactions between quinoline and PILs may also

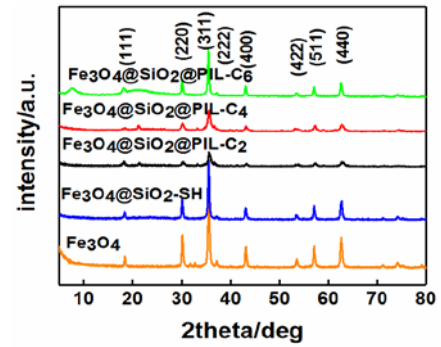

Fig. 6 *XRD spectra of Fe_3O_4, Fe_3O_4@SiO_2-SH and Fe_3O_4@SiO_2@PILs*

© The Institution of Engineering and Technology 2019

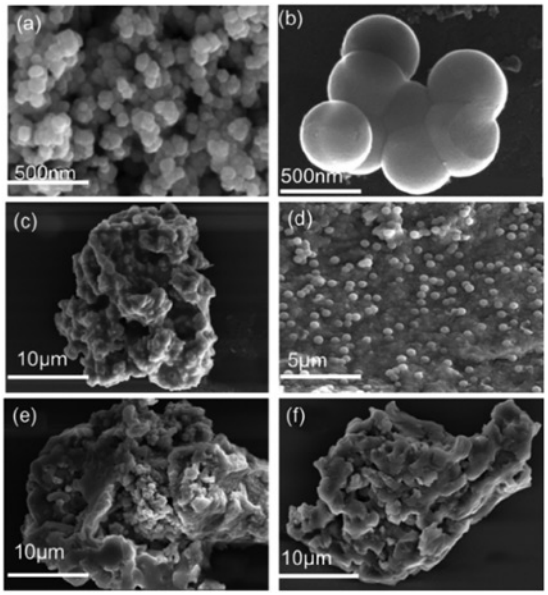

Fig. 7 *SEM images of*
a Fe_3O_4
b Fe_3O_4@SiO_2-SH
c Fe_3O_4@SiO_2@PIL-C_2
d Section of Fe_3O_4@SiO_2@PIL-C_2
e Fe_3O_4@SiO_2@PIL-C_4
f Fe_3O_4@SiO_2@PIL-C_6

Table 2 Denitrogenation efficiency of different N-compounds in simulated oils

Sorbent	Denitrogenation efficiency, %			
	Quinoline	Pyridine	Indole	Carbazole
Fe_3O_4@SiO_2@PIL-C_2	84.45	80.28	32.48	28.47
Fe_3O_4@SiO_2@PIL-C_4	84.16	79.16	30.87	24.15
Fe_3O_4@SiO_2@PIL-C_6	83.73	77.18	27.04	22.08

Denitrogenation conditions: adsorbent concentration 250 ppm, ratio of adsorbent to oil 1:10 (w/w), reaction time 5 min, temperature 25°C.

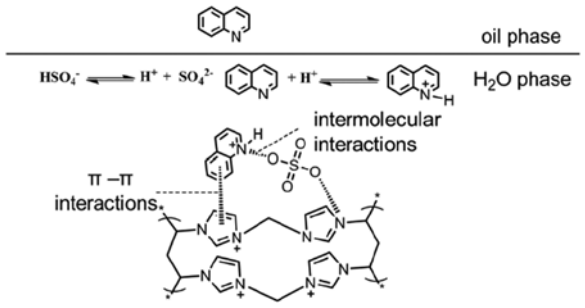

Fig. 8 *Possible mechanism of adsorption denitrification of simulated oil with Fe_3O_4@SiO_2@PILs*

play a positive role in the denitrogenation efficiency. A possible denitrogenation mechanism is shown in Fig. 8.

3.3. Effect of temperature on denitrogenation: The effect of adsorption temperature on the denitrification rate, with 1:10 of the ratio of reagent to oil (w: w) for 5 min, is described in Fig. 9.

Fig. 9 demonstrates that Fe_3O_4@SiO_2@PIL-C_2 has the highest denitrogenation efficiency in the three synthesised sorbents, and that the denitrogenation efficiency can be reduced with the increase of reaction temperature, ranging from 84.5 to 82.1% with the temperature rising from 30 to 70°C. The results interpret that the denitrogenation progress of ILs is an exothermic reaction, and high temperature will impact the activity of sorbent.

3.4. Effect of the ratio of sorbent on denitrogenation: The results of the ratio of sorbent to oil at 30°C and 5 min of reaction time are shown in Fig. 10. We can see that the denitrogenation efficiency of Fe_3O_4@SiO_2@PIL-C_2 decreases from 92.1 to 78.9% with the ratio decreased from 1:5 to 1:25, respectively. Similar results are observed for Fe_3O_4@SiO_2@PIL-C_4 and Fe_3O_4@SiO_2@PIL-C_6. This can be contributed by the increase of Fe_3O_4@SiO_2@PILs adsorption capacity to the N-compounds in diesel with the enhancement of the ratio of sorbent to oil.

3.5. Effect of reaction time on denitrogenation: Fig. 11 shows the effect of reaction time on denitrogenation at 30°C with a ratio of 1:5 sorbent to oil (w: w). The results in Fig. 11 indicate that the denitrogenation efficiency of Fe_3O_4@SiO_2@PIL-C_2 increases from 88.7 to 92.1% when the reaction time increases from 5 to 20 min, and that the denitrogenation rate may not show any obvious improvement for further adsorption time. Hence, a preferable adsorption time is 10 min.

As reported results in the literature, 95.9% of denitrogenation efficiency to quinoline was achieved by a non-magnetic IL formulated as [C_4mim]HSO_4 [33], while the denitrogenation efficiency of Fe_3O_4@SiO_2@PIL-C_2 to quinoline in this work is equally high up to 92.1%. Nevertheless, the magnetic composite proposed in this work possesses the advantage of simple and speed operation, and it can be easy to realise automation. It is obvious that a promising sorbent for denitrogenation to the N-compounds was developed in this work, especially for the basic N-compounds.

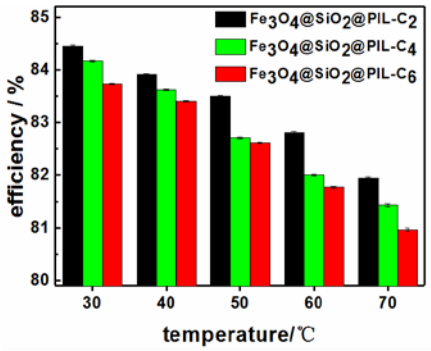

Fig. 9 *Effect of isotherms on denitrogenation rate over Fe_3O_4@SiO_2@PILs*

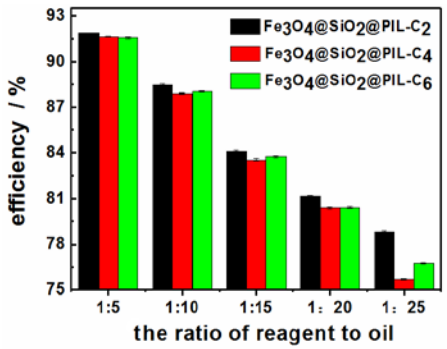

Fig. 10 *Effect of the ratio of sorbent to oil on denitrogenation rate over Fe_3O_4@ SiO_2@PILs*

© The Institution of Engineering and Technology 2019

doi: 10.1049/mnl.2019.0245

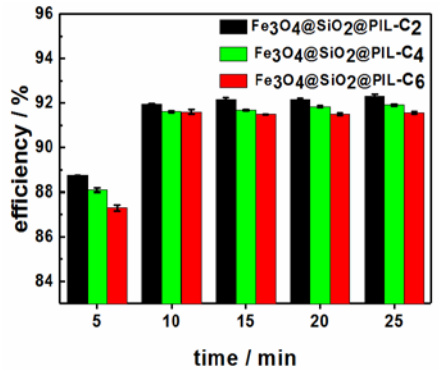

Fig. 11 *Effect of reaction time on denitrogenation rate over Fe_3O_4@SiO_2@PILs*

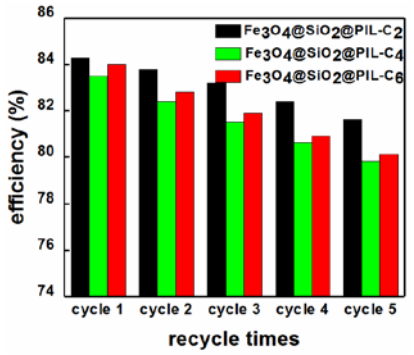

Fig. 12 *Effect of recycle times on denitrogenation rate over Fe_3O_4@SiO_2@PILs*

3.6. Effect of recycle times on denitrogenation of diesel: Based on the denitrogenation efficiency to quinoline in simulated oils, the denitrogenation experiments of the synthesised sorbents to diesel were carried out in the optimum denitrogenation conditions. Under the condition of temperature 30°C, the ratio of sorbent to oil (w: w) 1:5 with 5 min reaction time, the effect of recycle times on denitrogenation efficiency of diesel is shown in Fig. 12.

Fig. 12 demonstrated that with the cycle time increased, the denitrogenation efficiency of Fe_3O_4@SiO_2@PIL-C_2slightly decreased from 84.3 to 82.5%, which is much lower than the results of simulated oils in 92.1% denitrogenation efficiency. Both Fe_3O_4@SiO_2@PIL-C_4 and Fe_3O_4@SiO_2@PIL-C_6show the same consequence with the cycle times. This can be explained by two reasons, one is that there are some amounts of neutral N-compounds in the diesel which cannot be adsorbed well by the sorbents, and the other is the complexity composition of real oils which may be adsorbed on the surface of Fe_3O_4@SiO_2@PILs leading to decrease the sorbents effect.

4. Conclusions: The synthesis and denitrogenation of magnetic PILs to N-containing oils were investigated. Fe_3O_4@SiO_2@ PILs were synthesised by grafting PILs on the surface of silica-coated Fe_3O_4. Structural characterisation shows that Fe_3O_4@SiO_2@ PILs possess regular morphology, good stability and magnetic properties. Fe_3O_4@SiO_2@ PILs perform better denitrogenation efficiency of basic N-compounds than that of neutral N-compounds, and the shorter side alkyl chain in Fe_3O_4@SiO_2@ PILs will benefit the denitrogenation efficiency than the longer ones. The effects of temperature, reaction times, ratio of reagent to oil on denitrogenation for simulated oils and diesel were discussed. Denitrogenation efficiency of 92.1% to the simulated oils and 84.3% to diesel were achieved under the optimum condition. In addition, Fe_3O_4@SiO_2@ PILs can be used at least for five times without significant decreased of denitrogenation efficiency, which provides a more convenient recycling method with low consumption. It is suggested that magnetic PILs have a potential application in denitrogenation process as environment-friendly sorbent.

5. Acknowledgments: The work was supported by K. C. Wong Magna Fund of the Ningbo University. The authors are grateful to Science and Technology Program of Zhejiang (grant no. 2015C31044) and the Ningbo Natural Science Foundation (grant no. 2014A610113) for the financial support.

6 References

[1] Sunil K., Srivastava V.C., Nanoti S.M., *ET AL.*: 'Solvent evaluation for desulfurization and denitrification of gas oil using performance and industrial usability indices', *AIChE J.*, 2015, **61**, (7), pp. 2257–2267

[2] Ahmed I., Hasan Z., Khan N.A., *ET AL.*: 'Adsorptive denitrogenation of model fuels with porous metal-organic frameworks (MOFs): effect of acidity and basicity of MOFs', *Appl. Catal. B, Environ.*, 2013, **129**, pp. 123–129

[3] Ahmed I., Jun J.W., Jung B.K., *ET AL.*: 'Adsorptive denitrogenation of model fossil fuels with Lewis acid-loaded metal-organic frameworks (MOFs)', *Chem. Eng. J.*, 2014, **255**, pp. 623–629

[4] Klimov O.V., Nadeina K.A., Vatutina Y.V., *ET AL.*: '$CoMo/Al_2O_3$ hydrotreating catalysts of diesel fuel with improved hydrodenitrogenation activity', *Catal. Today*, 2018, **307**, pp. 73–83

[5] Lee K.S., Abe H., Reimer J.A., *ET AL.*: 'Hydrodenitrogenation of quinoline over high-surface-area Mo_2N', *J. Catal.*, 1993, **139**, (1), pp. 34–40

[6] Khan N.A., Yoo D.K., Jhung S.H.: 'Polyaniline-encapsulated metal-organic framework MIL-101: adsorbent with record-high adsorption capacity for the removal of both basic quinoline and neutral indole from liquid fuel', *ACS Appl. Mater. Interfaces*, 2018, **10**, (41), pp. 35639–35646

[7] Huo Q., Li J.S., Liu G.Q., *ET AL.*: 'Adsorption desulfurization performances of Zn/Co porous carbons derived from bimetal-organic frameworks', *Chem. Eng. J.*, 2019, **362**, pp. 287–297

[8] Yang H.W., Bai L.J., Wei D.L., *ET AL.*: 'Ionic self-assembly of poly(ionic liquid)-polyoxometalate hybrids for selective adsorption of anionic dyes', *Chem. Eng. J.*, 2019, **358**, pp. 850–859

[9] Ahmed I., Jhung S.H.: 'Remarkable improvement in adsorptive denitrogenation of model fossil fuels with CuCl/activated carbon, prepared under ambient condition', *Chem. Eng. J.*, 2015, **279**, pp. 327–334

[10] Hsu C.J., Chiou H.J., Chen Y.H., *ET AL.*: 'Mercury adsorption and re-emission inhibition from actual WFGD wastewater using sulfur-containing activated carbon', *Environ. Res.*, 2019, **168**, pp. 319–328

[11] Ge Y.H., Shu H., Xu X.Y., *ET AL.*: 'Combined magnetic porous molecularly imprinted polymers and deep eutectic solvents for efficient and selective extraction of aristolochic acid I and II from rat urine', *Mater. Sci. Eng. C, Mater. Biol. Appl.*, 2019, **97**, pp. 650–657

[12] Martínez Saavedra L.N., Penido R.G., de Azevedo Santos L., *ET AL.*: 'Molecularly imprinted polymers for selective adsorption of quinoline: theoretical and experimental studies', *RSC Adv.*, 2018, **8**, (50), pp. 28775–28786

[13] Song H.Y., You J.A., Li B., *ET AL.*: 'Synthesis, characterization and adsorptive denitrogenation performance of bimodal mesoporous Ti-HMS/KIL-2 composite: a comparative study on synthetic methodology', *Chem. Eng. J.*, 2017, **327**, pp. 406–417

[14] Shahriar S.A., Lin H.F., Zheng Y.: 'Adsorptive denitrogenation and desulfurization of diesel fractions by mesoporous SBA15-supported nickel(II) phosphide synthesized through a novel approach of urea matrix combustion', *Ind. Eng. Chem. Res.*, 2012, **51**, (44), pp. 14503–14510

[15] Mohammadian M., Ahmadi M., Khosravi-Nikou M.R.: 'Adsorptive desulfurization and denitrogenation of model fuel by mesoporous adsorbents (MSU-S and CoO-MSU-S)', *Pet. Sci. Technol.*, 2017, **35**, (6), pp. 608–614

[16] Ahmed I., Panja T., Khan N.A., *ET AL.*: 'Nitrogen-doped porous carbons from ionic liquids@MOF: remarkable adsorbents for both aqueous and nonaqueous media', *ACS Appl. Mater. Interfaces*, 2017, **9**, (11), pp. 10276–10285

[17] Li S.W., Yang Z., Gao R.M., *ET AL.*: 'Direct synthesis of mesoporous SRL-POM@MOF-199@MCM-41 and its highly catalytic performance for the oxidesulfurization of DBT', *Appl. Catal. B, Environ.*, 2018, **221**, pp. 574–583

© The Institution of Engineering and Technology 2019

[18] Songolzadeh M., Soleimani M., Ravanchi M.T.: 'Evaluation of metal type in MIL-100 structure to synthesize a selective adsorbent for the basic N-compounds removal from liquid fuels', *Microporous Mesoporous Mater.*, 2019, **274**, pp. 54–60
[19] Wang B., Qin L., Mu T., *ET AL.*: 'Are ionic liquids chemically stable?', *Chem. Rev.*, 2017, **117**, (10), pp. 7113–7131
[20] Melinda S., Steve G.: 'Ionic Janus liquid droplets assembled and propelled by electric field', *Angew. Chem., Int. Ed. Engl.*, 2018, **57**, (51), pp. 16773–16776
[21] Abro R., Abro M., Gao S.R., *ET AL.*: 'Extractive denitrogenation of fuel oils using ionic liquids: a review', *RSC Adv.*, 2016, **6**, (96), pp. 93932–93946
[22] Lui M.Y., Cattelan L., Player L.C., *ET AL.*: 'Extractive denitrogenation of fuel oils with ionic liquids: a systematic study', *Energy Fuels*, 2017, **31**, (3), pp. 2183–2189
[23] Wang H., Xie C.X., Yu S.T., *ET AL.*: 'Denitrification of simulated oil by extraction with $H_2PO_4^-$ based ionic liquids', *Chem. Eng. J.*, 2014, **237**, pp. 286–290
[24] Zhang C., Zhang W., Gao H., *ET AL.*: 'Synthesis and gas transport properties of poly(ionic liquid) based semi-interpenetrating polymer network membranes for CO_2/N_2 separation', *J. Membr. Sci.*, 2017, **528**, pp. 72–81
[25] Gomez I., De Anastro A.F., Leonet O., *ET AL.*: 'Sulfur polymers meet poly(ionic liquid)s: bringing new properties to both polymer families', *Macromol. Rapid Commun.*, 2018, **39**, (21), p. 1800529 (1800521–1800526)
[26] Ponkratov D.O., Lozinskaya E.I., Vlasov P.S., *ET AL.*: 'Synthesis of novel families of conductive cationic poly(ionic liquid)s and their application in all-polymer flexible pseudo-supercapacitors', *Electrochim. Acta*, 2018, **281**, pp. 777–788
[27] Zhao B., He M., Chen B., *ET AL.*: 'Ligand-assisted magnetic solid phase extraction for fast speciation of silver nanoparticles and silver ions in environmental water', *Talanta*, 2018, **183**, pp. 268–275
[28] Liang L., Wang X., Sun Y., *ET AL.*: 'Magnetic solid-phase extraction of triazine herbicides from rice using metal-organic framework MIL-101(Cr) functionalized magnetic particles', *Talanta*, 2018, **179**, pp. 512–519
[29] Tan P., Xie X.Y., Liu X.Q., *ET AL.*: 'Fabrication of magnetically responsive HKUST-1/Fe_3O_4 composites by dry gel conversion for deep desulfurization and denitrogenation', *J. Hazard. Mater.*, 2017, **321**, pp. 344–352
[30] Mirzaie A., Musabeygi T., Afzalinia A.: 'Sonochemical synthesis of magnetic responsive Fe_3O_4@TMU-17-NH_2 composite as sorbent for highly efficient ultrasonic-assisted denitrogenation of fossil fuel', *Ultrason. Sonochem.*, 2017, **38**, pp. 664–671
[31] Yin S., Sun J., Liu B., *ET AL.*: 'Magnetic material grafted cross-linked imidazolium based polyionic liquids: an efficient acid catalyst for the synthesis of promising liquid fuel 5-ethoxymethylfurfural from carbohydrates', *J. Mater. Chem. A*, 2015, **3**, (9), pp. 4992–4999
[32] Malihan L.B., Mittal N., Nisola G.M., *ET AL.*: 'Macroalgal biomass hydrolysis using dicationic acidic ionic liquids', *J. Chem. Technol. Biotechnol.*, 2017, **92**, (6), pp. 1290–1297
[33] Fan Y.C., Cai D.X., Zhang S.L., *ET AL.*: 'Effective removal of nitrogen compounds from model diesel fuel by easy-to-prepare ionic liquids', *Sep. Purif. Technol.*, 2019, **222**, pp. 92–98

© The Institution of Engineering and Technology 2019

doi: 10.1049/mnl.2019.0245